

# Coded Transmission in Synthetic Transmit Aperture Ultrasound Imaging Method

Ihor Trots, Yuriy Tasinkevych, Andrzej Nowicki and Marcin Lewandowski

**Abstract**—The paper presents the study of synthetic transmit aperture method applying the Golay coded transmission for medical ultrasound imaging. Longer coded excitation allows to increase the total energy of the transmitted signal without increasing the peak pressure. Signal-to-noise ratio and penetration depth are improved maintaining high ultrasound image resolution.

In the work the 128-element linear transducer array with 0.3 mm inter-element spacing excited by one cycle and the 8 and 16-bit Golay coded sequences at nominal frequencies 4 MHz was used. Single element transmission aperture was used to generate a spherical wave covering the full image region and all the elements received the echo signals. The comparison of 2D ultrasound images of the wire phantom as well as of the tissue mimicking phantom is presented to demonstrate the benefits of the coded transmission. The results were obtained using the synthetic aperture algorithm with transmit and receive signals correction based on a single element directivity function.

**Keywords**— Golay coded sequences, radiation pattern, synthetic aperture, ultrasound imaging.

## I. INTRODUCTION

THE ultrasound imaging has become much more prevalent than the other medical imaging techniques since it is more accessible, less expensive, safe, simpler to use and produces real-time images. However, to provide an accurate clinical interpretation the highest possible image quality is required. The most commonly used image quality measures are penetration depth, spatial resolution and image contrast. The penetration depth of the ultrasound image can be increased by applying longer signals and compressing them later on with the help of matched filter. The compressed signal is similar to that obtained using a single short pulse but with much higher amplitude. The spatial resolution of the ultrasound image can be improved by using the synthetic aperture (SA) method in which information is acquired simultaneously by small transmit-receive apertures placed in different positions and then used to reconstruct the full image from the collected data. In the simplest case a single element transmits an unfocused wave and then it is switched to receive the backscattered signal which yields a low resolution image line. Combining the data obtained from a large number of emissions one is able to obtain a high resolution image.

Authors are with the Institute of Fundamental Technological Research, Polish Academy of Sciences, Pawinskiego 5B, 02-106 Warsaw, Poland (corresponding author to provide phone: +48 22 826 12 81 ext.335; e-mail: igortr@ippt.gov.pl).

This work was supported by the Polish Ministry of Science and Higher Education (Grant NN518382137).

Till now, in the SA methods it is assumed that the transmit and receive elements are the point-like sources and the dynamical focusing is realized by finding the geometric distance from the transmitting element to the imaging point and back to the receiving element. But when the element size is comparable to the wavelength the influence of the element directivity on the wave field generation and reception becomes significant and if ignored might be a source of errors and noise artifacts in the resulting image. In this work the synthetic transmit aperture (STA) algorithm [1], which takes into account the single element directivity to improve the quality of the resulting image, is applied to reconstruct the ultrasound image.

The main objective of this work is to implement the STA method in ultrasound imaging where only one element transmits unfocused wave-field and all array elements receive the echo signals. The application of longer complementary Golay coded sequences allows to increase of the transmitted energy which improves the SNR and, as a result, the ultrasound image contrast.

The performed simulation was carried out using the *Field II* simulation program [2] in the MATLAB<sup>®</sup> environment. The 128-element linear transducer array with 0.3 mm pitch excited by a one cycle and the 8 and 16-bit Golay coded sequences at the nominal frequency of 4 MHz and the sampling rate of 40 MHz was used in the experiments. The comparison of 2D ultrasound images of the wire phantom and the tissue mimicking phantom is presented. The results show that using longer Golay coded sequences allows to increase penetration depth and image contrast maintaining spatial resolution.

## II. SYNTHETIC TRANSMIT APERTURE METHOD

STA method is a contrast to the conventional beamforming one, where only imaging along one line in receiving is used. In the STA method every image line is imaged as many times as the number of elements used. This will create an equal amount of low resolution images which are summed up to create one high spatial resolution image. This method is an alternative to conventional phased array. At each time a single array element transmits an ultrasound pulse and all elements receive the echo signals [3, 4]. The advantage of this approach is that a full dynamic focusing can be realized in both transmit and receive modes, giving the highest image quality.

The simple model for the STA ultrasound imaging is given in Fig. 1. In transmission only a single element is used. It creates a cylindrical wave (in the elevation plane the shape of the wavefront is determined by the height of the transducer) which covers the whole region of interest. The received echo

comes from all imaging directions, and the received signals can be used to create a whole image - in other words all of the scan lines can be beamformed in parallel. The created image has low resolution because there is no focusing in transmit, and therefore in the rest of this report it is called a low-resolution image. After the first low-resolution image, is acquired another element transmits and a second low-resolution image is created. After all of the transducer elements have transmitted, the low-resolution images are summed and a high-resolution image is created.

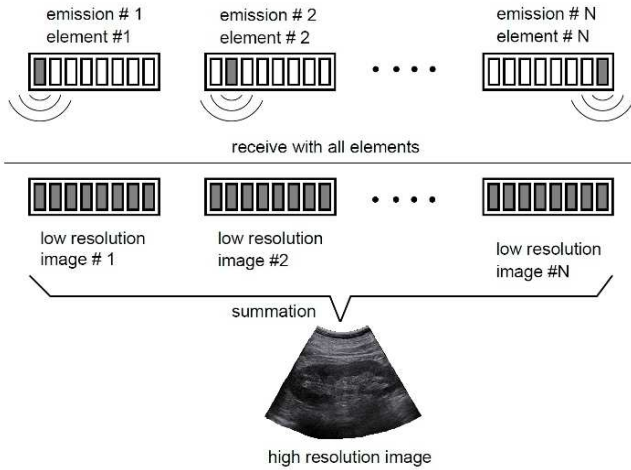


Fig. 1 Low-resolution images combined to produce a high resolution image

In the SA ultrasound imaging methods for each point in the resulting image every combination of transmit-receive pairs contributes according to the round-trip propagation time only. The angular dependence is not taken into account in the applied point-like source model. But when the width of the array element is comparable to the wavelength corresponding to the nominal frequency of the emitted signal, the point-like source model becomes inaccurate. Here, a STA imaging algorithm, which accounts for the element directivity function and its influence is applied [5].

The underlying idea can be illustrated on the following example, shown in Fig. 2. Here, it is assumed, that the same element transmits and receives signal. Two scatterers located at the points with polar coordinates  $(r_i, \theta_i)$ ,  $i=1,2$  such that  $r_{1m}=r_{2m}$  would contribute to the corresponding echo signal  $y_{m,m}(t)$  simultaneously, since the round-trip propagation time  $2r_{im}/c$ ,  $i=1,2$  is the same. Apparently, the contribution from the scatterer at the point  $(r_1, \theta_1)$  would be dominant, since the observation angle  $\theta_{1m}$  coincides with the direction of maximum radiation for the  $m$ -th element, whereas its transmit-receive efficiency at the angle  $\theta_{2m}$  is much smaller for the case of the scatterer at the point  $(r_2, \theta_2)$ . Thereby, evaluating the value of  $A(r_2, \theta_2)$ , the partial contribution of the echo  $y_{m,m}(t)$ , in addition to the correct signal from the obstacle located at  $(r_2, \theta_2)$  (being small due to the large observation angle  $\theta_{2m}$ ), would also introduce the erroneous signal from the scatterer located at  $(r_1, \theta_1)$ . The later signal is larger due to the small observation angle  $\theta_{1m}$ . The larger observation angles appear in

the imaging region close to the array aperture. Therefore, the most appreciable deviation from the point-like source model of the array element will occur there. A solution to the problem, which accounts for the observation angle in accordance with the array element directivity function, is proposed. Assume, that the dependence of the transmit-receive efficiency of a single array element on the observation angle is known and is denoted by  $f(\theta_m)$ , where  $\theta_m$  is measured from the line parallel to  $z$ -axis and passing through the  $m$ -th element center. Thus, in order to suppress the erroneous influence from the scatterer located at  $(r_1, \theta_1)$  on the value of the resulting signal  $A(r_2, \theta_2)$ , the partial contribution of the echo  $y_{m,m}(t)$  is weighted by the corresponding value of  $f(\theta_{2m})$ . This corresponds to the superposed signal correction in accordance with respective contributions of individual scatterers located at the points  $(r_1, \theta_1)$  and  $(r_2, \theta_2)$ .

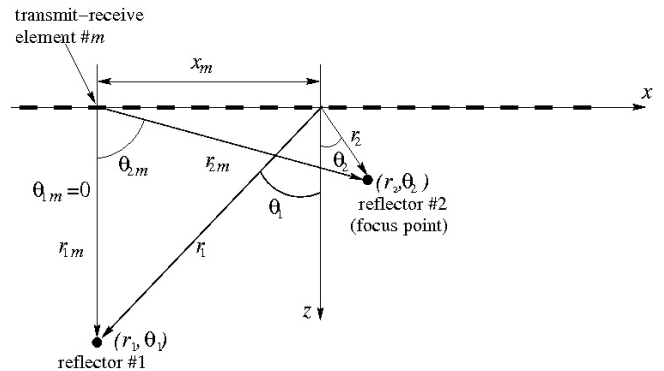


Fig. 2 Influence of the scatterer located at the point  $(r_1, \theta_1)$  on the value of resulting signal  $A(r_2, \theta_2)$  for imaging point  $(r_2, \theta_2)$

The above considerations lead to the following modification of the synthetic focusing imaging algorithm

$$A(r, \theta) = \sum_{m=1}^N \sum_{n=1}^N f(\theta_m) f(\theta_n) y_{m,n} \left( \frac{2r}{c} - \tau_{m,n} \right), \quad (1)$$

where  $\theta_i(r, \theta)$ ,  $i=m,n$  are the corresponding observation angles for the transmit-receive pair. The modification of the STA thus is expressed by a weighted summation of properly delayed RF signals (as in the case of conventional STA). The corresponding weights  $f(\theta_m)$ ,  $f(\theta_n)$  in the transmit and receive modes are calculated by means of the single element directivity function. Note, that the angles depend on the spatial location of the imaging point  $(r, \theta)$ . The directivity function  $f(\theta)$  can be calculated in the far-field approximation for a single element of the array transducer in analogous manner as in [6]

$$f(\theta) = \frac{\sin(\pi d / \lambda \sin \theta)}{\pi d / \lambda \sin \theta} \cos \theta, \quad (2)$$

where  $d$  is the element width, and  $\lambda$  is the wavelength.

### III. GOLAY COMPLEMENTARY SEQUENCES

Ultrasound imaging allows to visualize structures and organs in real-time, enabling an instantaneous evaluation of

clinical situation. But real problems appear when the reconstruction of the deeply located organs is needed. For that reason, coded excitation can be used making examination procedure more precise and allowing visualization of the deeply located organs in 2D B-mode ultrasound imaging.

Among the different excitation sequences proposed in ultrasonography, Golay codes evoke more and more interest in comparison with other signals. The reason of that lies in the fact that Golay codes, like no other signals, suppress to zero the amplitude of side-lobes. This type of complementary sequences has been introduced by Golay in the sixties [7]. In the seventies the Golay complementary codes were implemented using interdigital transducers accounting for the Doppler effect in surface acoustic waves (SAW) devices [8]. The pairs of Golay codes belong to a bigger family of signals, which consist of two binary sequences of the same length  $n$ , whose auto-correlation functions have the side-lobes equal in magnitude but opposite in sign. The sum of these auto-correlation functions gives a single auto-correlation function with the peak of  $2n$  and zero elsewhere [9].

Fig. 3 shows the pair of complementary Golay sequences, their autocorrelations, and the zero side-lobes sum of their autocorrelations.

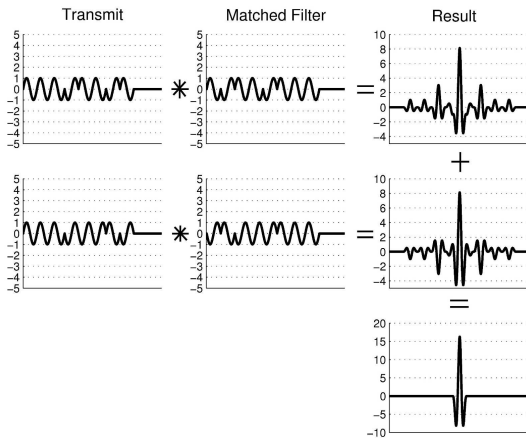


Fig. 3 Principle of side-lobes cancellation using pair of Golay complementary sequences of length 8 bits

IV. COMPUTER SIMULATION

All simulations in this work are carried out with a powerful software, *Field II*. The program is developed especially for investigating ultrasound fields, and gives the possibility to simulate and calculate ultrasound fields and defining one's own transducer. *Field II* is based on numerical analysis and runs under Matlab. The STA algorithm is used in the numerical examples presented in this paper.

To simulate a measurement numerous parameters have to be set. The transducer used in the measurements described later is the linear transducer L14-5/38. The parameters used in the simulations are similar to those of the transducer. The medium in the simulations is homogenous and such parameters as the attenuation and the speed of sound were set to be the same as in experiments. The numerical results presented in Fig. 4 were performed for a 128-element linear

transducer array with 0.3 mm pitch excited by one sine cycle burst pulse at a nominal frequency of 4 MHz. The element pitch is about  $\lambda$ , where  $\lambda$  corresponds to the nominal frequency of the burst pulse. The STA algorithm is employed. The transmit and receive elements combinations give a total of 128x128 possible RF A-lines. All these A-lines echo signals are sampled independently at a frequency of 40 MHz and stored in RAM.

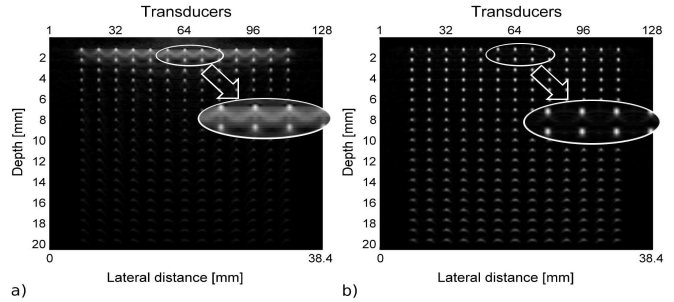


Fig. 4 Simulation of multi-point scatterers for 128-element linear array: a) not including directional diagram of element; b) including element directional diagram. Marked area is magnified evidencing suppression of the “noise”-like spatial variations of the scattered signal from the reflectors positioned near the transducer surface

The blurring of the scatterers placed near the aperture is significantly diminished in the case of introducing the directional diagram of element in synthetic focusing algorithm as compared to the algorithm without this correction

In Fig. 5 a computer simulation of multi-scatterers phantom when a 128-element linear transducer array was applied is shown. The one cycle as well as the pairs of complementary Golay sequences of the lengths 8 and 16 bits at nominal frequency 4 MHz were used. The phantom attenuation is equal to 0.5 dB/(MHz-cm). In the applied STA algorithm the element directivity correction scheme, discussed in [5], was implemented to improve the image quality near transducer aperture.

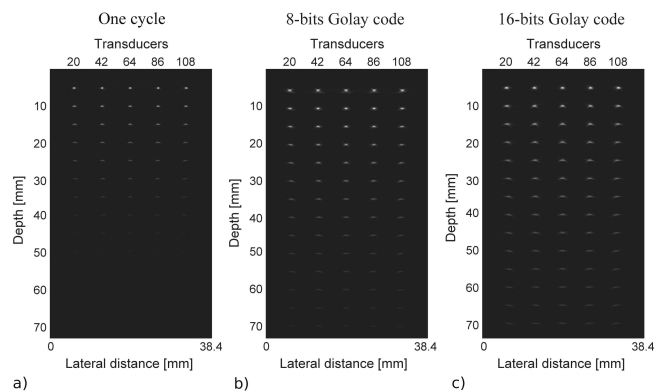


Fig. 5 Comparison of 2D ultrasound images obtained by computer simulation for 128-element linear array using: a) one cycle; b) 8-bit Golay sequences; c) 16-bit Golay sequences

The obtained 2D ultrasound images clearly demonstrate the advantage of using the Golay coded sequences. With the elongation of the coded sequences the acoustical energy

increases yielding a higher SNR, that leads to an increase in the penetration depth while maintaining both axial and lateral resolution. The latter depends on transducer acoustic field and is discussed in [10]. The visualization depth when the one cycle was applied is equal to about 3 cm (Fig. 5a), while in case of applying 8-bit Golay codes this depth increases to 5 cm (Fig. 5b), and for longer 16-bit Golay codes this depth of visualization increases up to 7 cm (Fig. 5c).

In order to compare the lateral resolution the cross section of phantom at a depths of 10 mm and 30 mm is shown in Fig. 6. Note, the normalization is perform with respect to the maximum values of the corresponding cross sections at different depth.

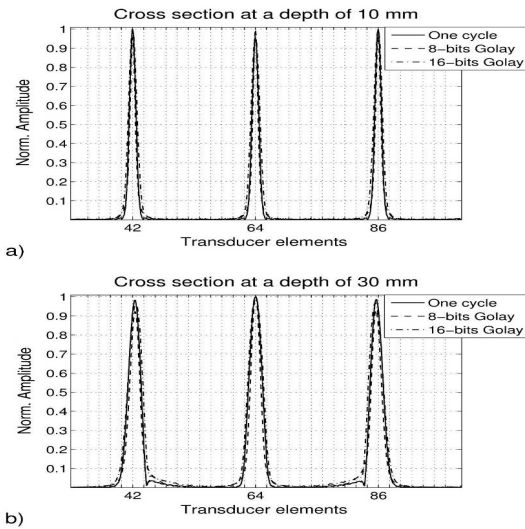


Fig. 6 Comparison of the lateral resolution at depths of 10 mm (a) and 30 mm (b) when one cycle, 8 and 16-bit Golay codes used

In Fig. 6 it can be seen that the lateral resolution at the different depths for all burst signals is the same. As anticipated, the lateral resolution illustrated in Fig. 6 as a function of depth is almost unchanged for the Golay codes of different length (being the function of the system bandwidth it is independent of the code duration [11]).

V. ULTRASOUND IMAGING SYSTEM

A simplified block diagram of the experimental setup used in this work is shown in Fig. 7.

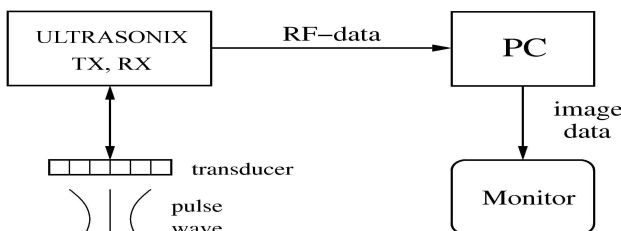


Fig. 7 Block diagram of the ultrasound imaging system

It's main part is an Ultrasonix - SonixTOUCH Research System (Ultrasonix Medical Corporation, Canada) equipped with a 128-element linear transducer array with 0.3 mm pitch.

Ultrasonix enables a full control of transmission and reception parameters for all 128 elements of the transducer. Besides, a full access to raw RF data enables one to send it to the PC for further digital processing. Next, the processed data are displayed on the monitor. All post processing and display is done on PC using Matlab®. The processing creates 2D ultrasound image focused in every point.

In synthetic aperture imaging all scan lines (full image) are created in each and every firing, while in standard beamforming only a single line is created. The amount of raw RF data needed in the STA algorithm for an *N*-element ultrasound transducer for reconstruction of a single image is proportional to  $D_{RF} * M * N$  and the number of delay-and-sum operations is  $D_{RF} * M * N^2$ , where  $D_{RF}$  is the number of samples in a single RF line. Thus, for the 128-element array, used in experiments, for 10 cm penetration ( $D_{RF} = 5500$  at 40 MHz sampling frequency) storage requirements is  $\approx 90 * 10^6$  samples or  $\approx 0.7$  Gb of RAM (for 8 bytes per sample in Matlab® double precision format). And the total number of delay-and-sum operations in the STA image reconstruction algorithm is  $\approx 11.5 * 10^9$ .

VI. EXPERIMENTAL RESULTS AND DISCUSSION

The 128-element linear transducer array excited by the 8 and 16-bit Golay coded sequences as well as a one cycle at nominal frequencies 4 MHz were used in the experiments. A single element in the transducer transmitting aperture was used to generate an ultrasound wave covering the full image region. All elements were used for both transmitting and receiving. The RF echo signals sampled independently at 40 MHz and processed by the STA algorithm. Experimental data were acquired by an Ultrasonix - SonixTOUCH Research System (Ultrasonix Medical Corporation, Canada).

The tissue mimicking phantom model 525 Danish Phantom Design with attenuation of background material 0.5 dB/(MHz-cm) was used. It consists of several nylon filaments twists 0.1 mm in diameter positioned every 1 cm axially. This phantom allows to examine the axial and lateral resolution at various depths in the ultrasound image.

The comparison of the 2D ultrasound images of the tissue phantom obtained for one cycle, 8-bit and 16-bit Golay complementary sequences is shown in Fig. 8. The peak pressure level of excitation signals at the transducer were set as low as possible to visually detect the echoes received using one cycle burst transmission slightly larger than the noise level. The same peak pressure has been used for the coded transmission. The obtained 2D ultrasound images show an excellent performance of the coded excitation in terms of increasing penetration depth. In the case of one cycle the penetration depth is equal only to 3cm (Fig. 8a). In the case of 8-bit Golay code the penetration depth increases up to 7 cm (Fig. 8b). With the elongation of the coded sequences to 16 bits the acoustical energy increases yielding higher SNR, that leads to an increase in the penetration depth up to 8 cm

(Fig. 8c). Note that axial and lateral resolution is the same for the all burst signals.

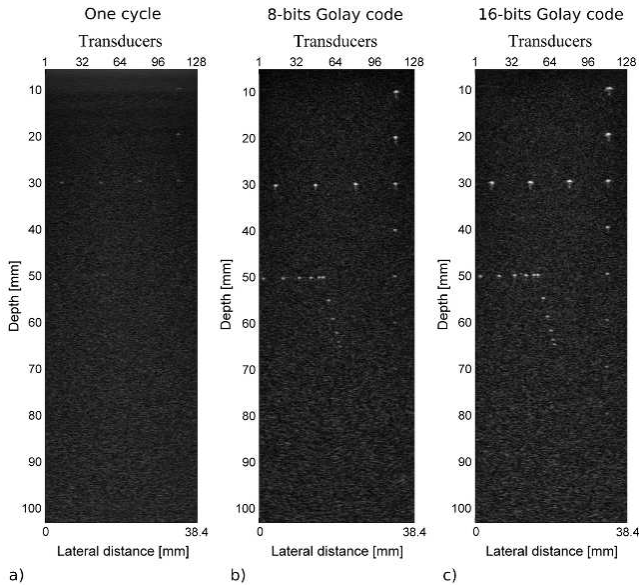


Fig. 8 2D ultrasound images of tissue mimicking phantom using: a) one cycle; b) 8-bit Golay code; c) 16-bit Golay code

In order to compare quantitatively the SNR gain the 112<sup>th</sup> line from 128 RF-lines of the 2D ultrasound images is shown in Fig. 9 and the SNR is calculated. For this purpose the noise level which appeared straight after the signal was chosen.

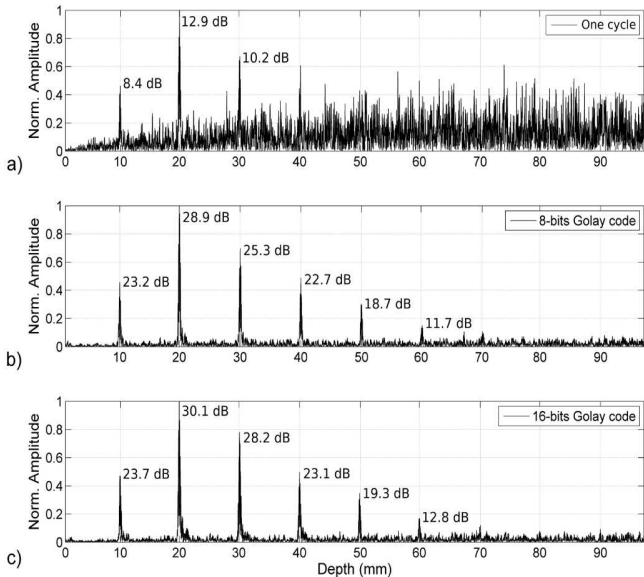


Fig. 9 The RF-lines of the tissue mimicking phantom using: a) one cycle; b) 8-bit Golay code; c) 16-bit Golay code

Fig. 9 shows that applying coded transmission in comparison to one cycle pulse allows to improve the SNR by about 15 dB. Elongating the coded transmission twice leads to the SNR increase by about 1.4 dB which is in agreement with the studies shown in [9] where the final output is  $2L$  times larger ( $L$  is the coded length) than the response to a single

impulse; however, the noise increases by a factor of  $\sqrt{2L}$  ( $\sqrt{L}$  for each correlation and  $\sqrt{2}$  for the addition).

Therefore, an improvement in the SNR of  $\sqrt{2L}$  is obtained in comparison with the single period burst transmission. More realistically, for transmit two sequences per observation time, the SNR improvement factor is  $\sqrt{L}$ . The SNR increase in its turn leads to improvement of the penetration depth and the contrast of the image.

The comparison of the B-mode images of the cyst phantom (model 571 Danish Phantom Design) with attenuation of the background material of 0.5 dB/(MHz-cm), and obtained for one cycle, 8-bit and 16-bit Golay code transmission is presented in Fig. 10. The phantom consists of a collection of cyst regions with the diameter 2, 4, and 8 mm distributed in depth which enables the evaluation of the contrast-to-noise ratio through the whole penetration depth. The same peak pressure has been used for all signal bursts.

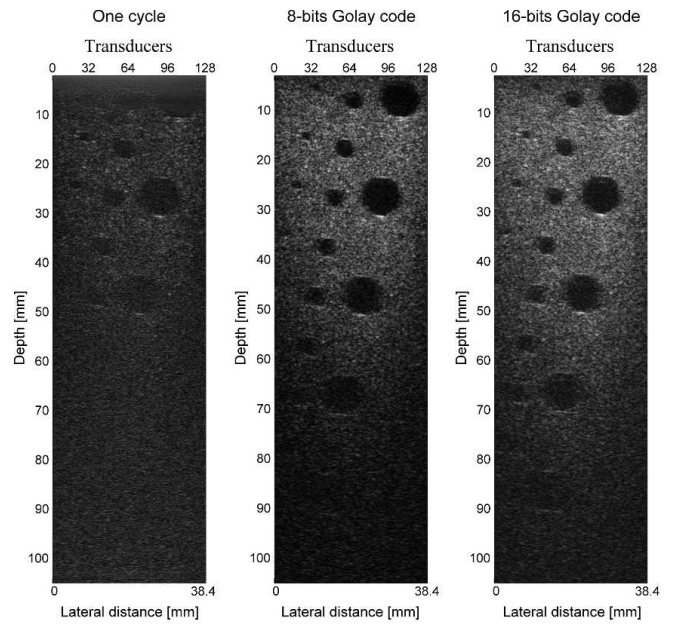


Fig. 10 2D ultrasound images of cyst phantom using: a) one cycle; b) 8-bit Golay code; c) 16-bit Golay code

The results in Fig. 10 demonstrate the benefits of applying the Golay coded transmission for ultrasound diagnostic i.e. the improved contrast in both the shallow and the deep region. The ultrasound penetration is nearly doubled for the 16-bit Golay codes in comparison with the single cycle transmission, effectively extending the diagnosable region in the practical medical application.

### VII. CONCLUSION

This work has addressed the problems in medical ultrasound imaging: improving of the penetration depth and gaining the SNR. To solve these problems, the complementary pairs of Golay coded sequences were used. The comparison of the 2D ultrasound images show that elongated coded sequences from 8-bits to 16-bits increase the penetration depth

by about 2 cm. Applying of the coded transmission in the STA method in a standard ultrasound scanner could allow improve the penetration depth and image contrast. Introduction of this method in medical ultrasound would increase the efficiency and quality of the ultrasound diagnostic.

Also the new algorithm based on the array element angular directivity function implementation into the conventional STA method and corresponding correction of the back-scattered RF signals of different transmit-receive pairs is presented. It is shown that the far-field radiation pattern of a narrow strip transducer, calculated for the case of a time harmonic uniform pressure distribution over its width, can serve as a good approximation for the above directivity function. The results of numerical calculations using simulated data have shown distinguishable improvement of the imaging quality of the scatterers situated in the region near the transducer aperture, the hazy blurring artefacts, observable in the case of conventional STA algorithm, are substantially suppressed.

#### REFERENCES

- [1] Y. Tasinkevych, A. Nowicki, I. Trots, "Element directivity influence in the synthetic focusing algorithm for ultrasound imaging," in *Proc. 57<sup>th</sup> Open Seminar on Acoustics*, Gliwice, Poland, 2010, pp. 197–200.
- [2] J.A. Jensen, "Linear description of ultrasound imaging systems," *Note for the International Summer School on Advanced Ultrasound Imaging*, Technical University of Denmark, June 10, 1999.
- [3] G.E. Trahey, L.F. Nock, "Synthetic receive aperture imaging with phase correction for motion and for tissue inhomogeneities — part I: Basic principles," *IEEE Trans. Ultrason. Ferroelec. Freq. Contr.*, vol. 39, no. 4, pp. 489–495, 1992.
- [4] I. Trots, A. Nowicki, M. Lewandowski, "Synthetic transmit aperture in ultrasound imaging," *Archives of Acoustics*, vol. 43, no. 4, pp. 685–695, 2009.
- [5] Y. Tasinkevych, I. Trots, A. Nowicki, P.A. Lewin, "Modified synthetic transmit aperture algorithm for ultrasound imaging," *Ultrasonics*, vol. 52, no. 2, pp. 333–342, 2012.
- [6] A.R. Selfridge, G.S. Kino, B.T. Khuri-Yakub, "A theory for the radiation pattern of a narrow-strip acoustic transducer," *Appl. Phys. Lett.*, vol. 37, no. 1, pp. 35–36, 1980.
- [7] M.J.E. Golay, "Complementary series," *IRE Tran. Inf. Theory*, vol. 7, pp. 82–87, 1961.
- [8] E.J. Danicki, "Complementary code realization based on surface acoustic waves," *Bulletin of Military Technical Academy*, vol. XXIII, no. 1, pp. 53–56, 1974.
- [9] I. Trots, A. Nowicki, W. Secomski, J. Litniewski, "Golay sequences – side-lobe canceling codes for ultrasonography," *Archives of Acoustics*, vol. 29, no. 1, pp. 87–97, 2004.
- [10] A. Nowicki, Z. Klimonda, M. Lewandowski, J. Litniewski, P.A. Lewin, I. Trots, "Direct and post-compressed sound fields for different coded excitation," *Acoustical Imaging*, vol. 28, pp. 399–407, 2007.
- [11] M. Xu, L.V. Wang, "Analytic explanation of spatial resolution related to bandwidth and detector aperture size in thermoacoustic or photoacoustic reconstruction," *Phys. Rev. E*, vol. 67, no. 5, pp. 1–15, 2003.